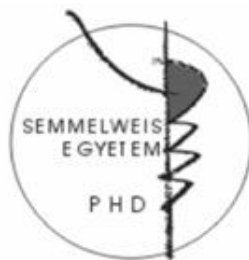


Disturbance of cardiac intracellular calcium ion
homeostasis in primary dilated and diabetic
cardiomyopathy

Ph.D. Thesis

Kemecsei Péter Imre MD, DMD

Semmelweis University
Basic Medicine Doctoral School



Supervisor: Ivanics Tamás, senior associate professor, MD, Ph.D.

Official reviewers:

Violetta Kékesi, senior associate professor, MD, Ph.D.

Gyula P Szigeti, department head, MD, Ph.D.

Head of the Final Examination Committee :

Gábor Pavlik, professor, MD, Ph.D.

Members of the Final Examination Committee:

Péter Várnai, senior associate professor, MD, Ph.D.

Ágnes Angyalné Pataki, electrophysiologist, MD, Ph.D.

Budapest

2013

Introduction

Due to the increasing prevalence of heart failure in our society, we set primary and secondary cardiomyopathies in the focus of our interest. The primary and secondary forms can be distinguished based on the etiology of the cardiomyopathic disorder. We studied a transgenic model of primary cardiomyopathy which was developed by Arber and colleagues and is characterized by a deficiency in muscle LIM protein (MLP-KO), a striated muscle-specific Lim-only protein. This transgenic experimental model shares common features of human dilated cardiomyopathy. The importance of the MLP-KO model is underlined by the clinical observation that mutations of Z-disk proteins, including MLP, eventually result in overt cardiomyopathy in humans.

For the model of secondary cardiomyopathy a metabolic syndrome induced cardiomyopathy was chosen. Metabolic syndrome is a complex metabolic disorder which is characterized by the constellation of obesity, insulin resistance, hypertension and dyslipidaemia. The prevalence of the disorder has increased considerably worldwide over the past few decades. The syndrome and its various components have been associated with increased risk for cardiovascular diseases, heart failure and mortality. Metabolic alterations related to the metabolic syndrome including dyslipidaemia, failing insulin action and consequential hyperglycemia result in complex disturbances of cardiomyocyte metabolism, which can bring about the development of cardiac dysfunction and ultimately heart failure. Coexisting vascular dysfunction, coronary artery disease and hypertension further aggravate cardiac dysfunction. Comprehensive description of cardiac intracellular calcium (Ca^{2+}_i) handling in metabolic syndrome where several pathophysiological factors act cooperatively on the heart is scarce in the literature. The high fructose intake induced metabolic changes in rats provide a proper model to mimic human metabolic syndrome, because of the presence of insulin resistance, hypertension and dyslipidaemia.

It is generally accepted that in the failing heart alterations of Ca^{2+}_i handling substantially contribute to impaired cardiac performance. Diminished sarcoplasmic reticulum Ca^{2+} -ATPase (SERCA2a) and ryanodin receptor (RyR2) functions, alterations of SERCA2a,

phospholamban (PLB) and Na^+ - Ca^{2+} exchanger (NCX) expressions have been reported in the human failing heart and various experimental heart failure models. Investigations in previous models were performed in isolated cardiomyocyte experiments where the interpretation of functional and Ca^{2+}_i homeostasis related findings has serious limitations as opposed to in vivo and isolated heart experimental designs which create a more physiological environment. Beyond these, little is known about the early changes in Ca^{2+}_i cycling processes in heart failure and their time relation to the onset of cardiac dysfunction.

Aims

Our main goal was to investigate Ca^{2+}_i homeostasis, and its relation with hemodynamic function in primary and secondary cardiomyopathy.

We hypothesized that adaptive changes of cardiac intracellular calcium (Ca^{2+}_i) handling might compensate hemodynamic dysfunction and Ca^{2+}_i homeostasis disorders observed in young MLP-KO animals. Three and 9 months old mice were used to investigate the induction of a time related adaptive process.

Since various components of metabolic syndrome associate with cardiac intracellular calcium mishandling, a precipitating factor in the development of heart failure we aimed to provide a thorough description of early stage Ca^{2+}_i cycling alterations in the fructose-fed rat, an experimental model of the disorder, where insulin resistance, hypertension and dyslipidemia act cooperatively on the heart.

Materials and methods

Animal model of MLP-KO

MLP-deficient mice were examined at the age of 3 and 9 months. The background strain to the MLP^{-/-} mice was a hybrid cross of 129/Sv and C57BL/6 strains. The breeding pairs were a generous gift by L. J. De Windt (Department of Cardiology, Cardiovascular Research Institute Maastricht, University of Maastricht, the Netherlands). Age-matched wild type mice were used as controls. The animals were bred in our animal facility under SPF conditions. The mice were maintained at a 12-hour light and 12-hour dark cycle with free access to food and water. Tail tip DNA-test was performed with PCR technology in one randomly selected mouse from each MLP-KO litter to confirm the presence of homozygote genotype for the modified MLP allele. Experiments on animals followed the Guide for the Care and Use of Laboratory Animals published by the US National Institutes of Health (NIH Publication No. 85-23, revised 1996). The study protocol was approved by the Laboratory Animals Committee of the Semmelweis University of Budapest.

Animal model of metabolic syndrome

Male Sprague-Dawley rats at the age of 5 weeks were fed with fructose-rich diet for 6 weeks in which 66.8% of total calories was provided by fructose. Age matched control rats received control diet recommended by the manufacturer, in which protein, carbohydrate and fat contents were adjusted to the values of the research diet. The animals were kept in a facility with 12-hour light and 12-hour dark cycle with free access to food and water. Experiments on animals followed the Guide for the Care and Use of Laboratory Animals published by the US National Institutes of Health (NIH Publication No. 85-23, revised 1996). The study protocol was approved by the Laboratory Animals Committee of the Semmelweis University of Budapest.

At the end of the 6-week period animals were anesthetized by 40 mg/kg i.p. pentobarbital (Nembutal-Sanofi, Budapest, Hungary) and echocardiography was performed to evaluate heart dimensions and in vivo left ventricular functions. Echocardiography was followed by the measurement of blood pressure levels with the help of a catheter inserted into the carotid artery connected to a pressure transducer. Blood samples were also collected to determine plasma triglyceride levels.

In order to assess the diabetic status of the rats a subset of the animals were fasted overnight and subjected to an oral glucose tolerance test (oGTT) after echocardiography. 2 mg/kg glucose in 40% solution was administered via gastric gavage after obtaining a blood sample for control measurement from a line placed into the jugular vein. Blood glucose levels were measured in every 30 minutes.

Langendorff heart preparation - Indo-1 AM loading and fluorescence measurement

At 3 and 9 months of age, the animals were anesthetized by 40 mg/kg i.p. pentobarbital. Hearts were quickly excised and mounted on a Langendorff perfusion apparatus and perfusion was initiated with a modified Krebs-Henseleit solution, which was equilibrated with 95% O₂ and 5% CO₂. The temperature of the buffer was maintained at 37°C and pH was adjusted to 7.4. The perfusion pressure was set to 70 mmHg. Left ventricular pressure was registered by inserting a balloon catheter in the left ventricle, and coronary flow was measured by an ultrasonic transducer inserted in the perfusion line.

Hearts were loaded with 6.25 μM Indo-1 AM and were illuminated at 355 nm by a mercury arc lamp. The light emitted by Indo-1 was recorded at 400 nm (Ca²⁺_i-bound dye) and 506 nm (Ca²⁺_i-free dye) using a custom-made fluorometer. The fluorescence signals and the hemodynamic parameters were recorded and stored for off-line analysis.

After loading of Indo-1 the perfusate was supplemented with 0.6 mM probenecid to prevent dye-leakage from cardiomyocytes. After 15 min of dye-washout, the fluorescence signals were recorded in the basal state. Thereafter, the hearts were challenged with 5.0 nM isoproterenol infused via the aortic line. Heart rate, systolic and diastolic pressure stabilized in

about 5 min after the onset of infusion, at which stage the fluorescence signals were recorded. Cessation of isoproterenol infusion was followed by a 20 min stabilization period. After reaching control hemodynamic values, infusion with the SERCA2a inhibitor cyclopiazonic acid (CPA, 5 μ M) was started. At steady state of CPA administration, the parameters were recorded again. Administration of isoproterenol infusion was applied only in MLP-KO experiments.

Echocardiography

Transthoracic echocardiography was performed at the end of the 6-week diet period under 40 mg/kg i.p. pentobarbital anaesthesia with a SONOS 5500 ultrasound machine (Hewlett Packard) equipped with a high frequency linear transducer (5-15MHz). Long-axis B-mode images of the left ventricle were obtained to calculate end-diastolic volume (EDV) and end-systolic volume (ESV) from left ventricular area (LVA) and left ventricular length (LVL) as $8(LVAd)^2/3\pi LVLd$ and $8(LVAs)^2/3\pi LVLs$, respectively (d represents diastole and s represents systole). From these parameters ejection fraction was determined as $100(EDV-ESV)/EDV$. Diastolic left ventricular wall thickness was defined from short-axis echocardiograms of the left ventricle taken at the level of the papillary muscles. In order to assess fractional shortening (FS) short-axis images were used to measure left ventricular internal diameters in diastole and systole (LVIDd and LVIDs, respectively). These parameters allowed calculation of FS using the formula $100(LVIDd-LVIDs)/LVIDd$.

Data analysis and interpretation

Ca^{2+}_i -transients were obtained by the ratiometric technique from 400 and 506 nm signals. Prior to calculation, the individual fluorescence signals were corrected for closed shutter background and tissue autofluorescence of the unloaded tissue (correction for redox changes of $NAD(P)^+/NAD(P)H$). Changes of autofluorescence caused by the experimental interventions were tested in 3 unloaded hearts, but autofluorescent signals did not alter

significantly from baseline values at either wavelength throughout the experimental procedure.

Ca^{2+}_i -concentration ($[\text{Ca}^{2+}]_i$) was calculated with the formula determined by Grynkiewicz and colleagues. The Indo-1 dissociation constant (K_d) for calcium was determined previously at 844 nM. The fluorescent ratios at zero $[\text{Ca}^{2+}]_i$ (R_{\min}) and at saturating $[\text{Ca}^{2+}]_i$ (R_{\max}) were determined in separate experiments. Three mouse and three rat hearts loaded with Indo-1 were treated with 20 μM BAPTA-AM to define R_{\min} and 3-3 separate hearts were infused with 1 μM 4-bromo-calcium-ionophore (A23187) to determine R_{\max} . The calcium transient was assessed to determine systolic and diastolic $[\text{Ca}^{2+}]_i$ and Ca^{2+}_i -amplitude. Maximal rates of rise of $[\text{Ca}^{2+}]_i$ ($+d[\text{Ca}^{2+}]_i/dt_{\max}$) and decline of $[\text{Ca}^{2+}]_i$ ($-d[\text{Ca}^{2+}]_i/dt_{\max}$) were obtained as indices for the rate of Ca^{2+} release from and sequestration back into the SR, respectively.

Estimation of kinetic parameters of SR Ca^{2+} -transporters

In the metabolic syndrome model, using a computational model of Ca^{2+}_i handling in the cardiac myocytes, we estimated the kinetic parameters of Ca^{2+}_i handling proteins. From every data set, representative Ca^{2+}_i transients were selected with approximately constant end-diastolic Ca^{2+}_i level. The model state equation was then solved and numerical minimization of the squared error between model output and experimental $[\text{Ca}^{2+}]_i$ was used to estimate the unknown model parameters with non-negative constraints. The following kinetic parameters were estimated: k_{ch} [nMs^{-1}] represented the maximal rate of Ca^{2+} influx through the ryanodine channel, $t_{0.5}$ [ms] was the moment at which half of the maximal flux through RyR2 was reached, and was used as an index for RyR2 gating, V_{\max} ($[\text{nMs}^{-1}]$) is the maximum Ca^{2+} uptake rate into the SR by SERCA2a and k_m ([nM]) is the Michaelis-Menten constant of SERCA2a.

RNA isolation, Reverse transcription, Quantitative Real-Time PCR (qPCR)

Tissue samples of the left ventricle were pulverized under liquid nitrogen. As internal control, the transcript of glyceraldehyde 3-phosphate dehydrogenase (GAPDH) was determined. Na⁺-Ca²⁺ exchanger (NCX), ryanodin channel (RyR2), sarcoplasmic reticulum Ca²⁺ ATPase (SERCA2a) and phospholamban protein level were assessed.

Western blot analysis

Left ventricular tissue samples were pulverized in liquid nitrogen and aliquots of tissue powder were suspended in ice-cold Tris-EDTA buffer in both type of experiments. Densitometric values of several (n=3–5) independent experiments were averaged. Na⁺-Ca²⁺ exchanger (NCX), ryanodin channel (RyR2), sarcoplasmic reticulum Ca²⁺ ATPase (SERCA2a), phospholamban protein level (PLB) and phosphorylated phospholamban protein level (P-PLB, exclusively in fructose fed rats) were estimated. The expression of GAPDH was checked as internal control.

Results

MLP-KO mice

Survival rate, heart and body mass

Approximately 60% of the MLP-KO animals died within 7 days after birth (early phenotype) in contrast to controls (15% death rate). The remaining MLP-KO animals, which belonged to the adult phenotype, developed and behaved similarly to the control animals: on the average, less than 10% of MLP-KO and controls were lost between 7 days and 9 months

after birth. The surviving male animals were included in the experiments at 3 and 9 months of age. All randomly selected MLP-KO mice proved to be homozygous for the mutant MLP gene on basis of the tail tip DNA test.

Heart and body mass did not differ significantly between control and MLP-KO mice either at 3 or 9 months of age. The ratio of heart to body mass, calculated as an index of cardiac hypertrophy, was not different between control and MLP-KO animals at either age.

Hemodynamic function of isolated perfused hearts

Under unchallenged conditions, heart rate, left ventricular developed pressure, end-diastolic pressure and contractility ($+dP_{IV}/dt_{max}$) did not differ among the groups studied. However, the lusitropic function ($-dP_{IV}/dt_{max}$) of 3-months old MLP-KO hearts was diminished when compared to control hearts of the same age. This difference could not be observed when comparing hearts of 9-months old MLP-KO with corresponding controls. Coronary flow was significantly higher both in the 3- and 9-months old MLP-KO hearts relative to age-matched controls.

The β -adrenergic agonist isoproterenol (5.0 nM) produced significant elevation in heart rate, $+dP_{IV}/dt_{max}$ and $-dP_{IV}/dt_{max}$. No differences between MLP-KO hearts and controls could be identified. Isoproterenol infusion hardly affected coronary flow compared to the unchallenged conditions with the exception of a small, but significant increase in the 3-months old MLP-KO hearts.

Exposure to the SERCA2-blocker CPA resulted in a significantly higher rise in end-diastolic left ventricular pressure in 3-months old MLP-KO hearts than in age-matched controls (85% and 14%, respectively). This difference in response completely disappeared in the hearts at 9-months of age. CPA affected developed pressure also more severely in the 3-month old hearts compared to age-matched controls. The same was true for the decline in $+dP_{IV}/dt_{max}$, and $-dP_{IV}/dt_{max}$ in CPA-treated, 3-month old hearts. CPA challenge significantly decreased coronary flow in all experimental groups, whereas this intervention did not affect the difference between control and age-matched MLP-KO hearts.

Intracellular Ca²⁺ cycling

In unchallenged hearts, all characteristic parameters of the Ca²⁺_i-transient had similar values in MLP-KO and age-matched controls, both in the 3- and 9-month old hearts. During isoproterenol stimulation, end-diastolic Ca²⁺_i concentration, and both maximum rate of rise of Ca²⁺_i (+dCa²⁺_i/dt_{max}) and maximum rate of Ca²⁺_i decline (-dCa²⁺_i/dt_{max}) were significantly elevated in the hearts of each groups. No differences in response between control and MLP-deficient hearts could be observed.

Exposure to CPA induced a significant elevation of end-diastolic Ca²⁺_i concentration in each of the studied groups. It is of note that the increase in end-diastolic Ca²⁺_i levels in the 3-month old MLP-KO group significantly exceeded that of age-matched control hearts during CPA administration (238% and 112%, respectively). The striking difference in response to CPA between MLP-KO and controls disappeared at 9 months of age. CPA infusion significantly decreased +dCa²⁺_i/dt_{max} in all but the 9-month old MLP-KO hearts. Moreover, -dCa²⁺_i/dt_{max} was significantly reduced in 3-month old MLP-KO CPA-treated hearts; this effect was absent in 9-month old hearts.

mRNA and protein levels of proteins involved in Ca²⁺ cycling

The GAPDH-normalized mRNA expression of the major sarcoplasmic reticular Ca²⁺-releasing channel, RyR2, did not differ between 3-month old control and MLP-KO animals. At the age of 9 months, RyR2 mRNA level showed a minor, albeit significant reduction in MLP-KO hearts. In contrast, the RyR2 protein content was neither significantly different between the two 3-months old groups nor between the two 9-month old groups.

Amongst the Ca²⁺-sequestering transporters, NCX mRNA expression was similar in each of the studied groups. The tissue protein content of NCX was also not statistically different between the various groups.

In contrast, mRNA expression levels of SERCA2a were significantly lower in hearts of

3-month old MLP-KO mice than in age-matched control hearts. The SERCA2a mRNA expression in the 9-month old MLP-KO mice was significantly higher than that in the 3-months old MLP-KO animals and the difference between controls and MLP-KO hearts disappeared. A similar pattern of change was observed in protein levels. The SERCA2a protein concentration was also significantly lower in 3-month old MLP-KO hearts compared with corresponding, age-matched controls. A considerable (although not significant, i.e., $p=0.07$) 60% increase was observed in cardiac SERCA2a protein levels of 9-month old MLP-KO rats compared with corresponding 3-month old animals. The SERCA2a protein expression did not significantly differ between 9-month old MLP-KO hearts and age-matched controls, strongly suggesting that SERCA2a normalized in 9-month old MLP-deficient animals both at the mRNA and protein levels.

Similarly to the SERCA2a mRNA and protein expression, the mRNA and protein levels of PLB were lower in 3-month old MLP-KO mice than in age-matched controls. Increased PLB expression was observed in hearts of 9-month old MLP-KO mice compared to the 3-month old hearts. This alteration was reflected by both mRNA and protein data. In 9-month old MLP-KO hearts PLB mRNA and protein concentrations exceeded those measured in age-matched control animals.

Fructose fed rats

General data

Fructose-fed rats had similar body mass as controls, while their heart weight exceeded that of rats kept on normal chow. Therefore, the ratio of heart to body mass, calculated as an index of cardiac hypertrophy was higher in animals with metabolic syndrome. Mean arterial pressure and serum triglyceride level were also elevated after 6 weeks of fructose feeding. Although fasting blood glucose levels did not differ between the studied groups, oral glucose tolerance test (oGTT) revealed the presence of insulin resistance in the fructose-fed animals,

showing that the elevation of blood glucose level was more pronounced in this group, and did not return to fasting levels during the examination period of 2 hours compared to control rats.

Echocardiographic measurements

Morphological analysis of the left ventricle showed thickening of the interventricular septum (IVSd), and increased end-diastolic volume in the hearts of fructose-fed animals. The dynamic parameters describing left ventricular contractile performance revealed that stroke volume was elevated in the hearts of rats with metabolic syndrome, whereas the values of ejection fraction (EF) and fractional shortening (FS) were normal both in the control and diseased animals.

Hemodynamic function of isolated hearts

Under basal conditions developed pressure, heart rate, end diastolic pressure, and $+dP/dt_{\max}$ and $-dP/dt_{\max}$ characterizing inotropic and lusitropic function, respectively, did not show difference between the control and fructose-fed groups. However, coronary blood supply to the cardiac tissue was diminished in the diseased hearts at rest. Administration of 5 μM CPA induced a significant reduction in developed pressure, heart rate and coronary flow in both experimental groups, but the response in developed pressure elicited in hearts of the fructose-fed rats was more prominent. This enhanced sensitivity of the diseased hearts to SERCA2a inhibition was also evidenced by the higher end-diastolic pressure, and reduced $+dP/dt_{\max}$ and $-dP/dt_{\max}$ values recorded after CPA treatment.

Intracellular Ca^{2+} cycling

Under basal condition, no differences could be observed in end-diastolic Ca^{2+}_i levels and $+d\text{Ca}^{2+}_i/dt_{\max}$ between the two experimental groups. However, $-d\text{Ca}^{2+}_i/dt_{\max}$ and half decay time of the Ca^{2+}_i transient (DT_{50}) indicating the rate of Ca^{2+} sequestration into the SR

were reduced in the animals with metabolic syndrome at rest. Depressed Ca^{2+} sequestration resulted in the reduction of Ca^{2+}_i transient amplitude. CPA administration resulted in an elevation of end-diastolic Ca^{2+}_i levels, whereas Ca^{2+}_i transient amplitude, DT_{50} , and $+\text{dCa}^{2+}_i/\text{dt}_{\text{max}}$ and $-\text{dCa}^{2+}_i/\text{dt}_{\text{max}}$ from and to the SR, respectively, were depressed in both groups compared to basal values. Processes of the intracellular Ca^{2+} cycling of the hearts of the fructose-fed rats were more vulnerable to SERCA2a inhibition. This observation was underlined by the greater increase in end-diastolic Ca^{2+}_i levels, the more pronounced reduction in $+\text{dCa}^{2+}_i/\text{dt}_{\text{max}}$, the smaller Ca^{2+}_i transient amplitude and the significantly slower rate of Ca^{2+} removal from the cytosol ($-\text{dCa}^{2+}_i/\text{dt}_{\text{max}}$, DT_{50}) in response to CPA application in the hearts of rats with metabolic syndrome. These CPA induced changes in Ca^{2+}_i handling were also reflected by analogous alterations in the hemodynamic parameters of the diseased hearts.

Kinetic parameters of SR Ca^{2+} transporters (k_{ch} and $t_{0.5}$ of RyR2, and V_{max} and k_{m} of SERCA2a) were estimated by fitting the computational model to the Ca^{2+}_i transients as described above. Model fitting showed that the rate of Ca^{2+} flux through RyR2 (k_{ch}) was similar in the healthy and diseased hearts. Although RyR2 conductance decreased in both experimental groups after CPA administration, the value of k_{ch} became significantly lower in the fructose-fed group upon SERCA2a inhibition. The values of model parameter $t_{0.5}$ of RyR2 were similar in control and fructose-fed hearts and were not influenced by CPA treatment in either groups. The parameter estimation of SERCA2a pump activity showed that V_{max} was significantly higher under basal conditions and responded to CPA administration more sensitively in the metabolic syndrome group. This enhanced response was demonstrated by the disappearance of the significant difference between the two groups. k_{m} of the SERCA2a pump was elevated in diseased hearts. Upon CPA administration the affinity of SERCA2a for Ca^{2+} considerably decreased in both groups, but k_{m} remained significantly higher in the metabolic syndrome group as compared to control hearts.

Protein expression of Ca²⁺ cycling key enzymes

The expression of the SR Ca²⁺ releasing channel RyR2 in the hearts of fructose-fed rats was similar compared to that of control hearts. Among the Ca²⁺ eliminating enzymes the expression of NCX was unaffected by fructose diet. The protein level of SERCA2a pump however showed several fold elevation in the diseased hearts. In case of the major SERCA2a regulator protein phospholamban (PLB) a similar level of expression was observed in both groups. However, the level of Ser16 phosphorylated PLB (P-PLB) in the cardiac tissue of fructose fed rats exceeded substantially the control values.

Conclusion

In a model of primary dilatative cardiomyopathy, the 3-month old MLP-deficient hearts showed a transitory dysfunction in Ca²⁺_i handling, which was rescued by compensatory mechanisms later in life. These mechanisms may exert a beneficial effect on cardiomyocyte Ca²⁺_i homeostasis and, hence, contractile properties, as seen in hearts of 9-month old MLP-KO mice. The beneficial mechanisms might involve the normalized expression of SERCA2a in the affected heart. The present findings also indicate a transient decline in the contractile efficiency of the hearts of surviving MLP-deficient mice. Overall, age-related alterations in cardiac Ca²⁺_i handling might offer a potential adaptive process to rescue MLP-KO mice from early heart failure.

In the high fructose fed rat experiments, we have provided evidence that the primary sign of impaired myocardial Ca²⁺_i handling is the decline of Ca²⁺ sequestering processes which is the direct consequence of disturbed SERCA2a function. This SERCA2a dysfunction is most probably the result of imbalances of metabolic pathways within the cardiomyocytes and a concomitantly enhanced oxidative stress. The disturbance of SERCA2a activity recruits compensatory mechanisms which include upregulation of SERCA2a transporter expression and pathways responsible for PLB phosphorylation. These compensatory alterations tend to

normalize Ca^{2+}_i cycling, consequently at this stage of the disease overt cardiac dysfunction cannot be observed under resting conditions. However, this delicate equilibrium is clearly vulnerable to a further decline in SERCA2a function.

Own publications

Publications related to thesis

Kemecsei P, Miklós Zs, Bíró T, Marincsák R, Tóth BI, Komlódi-Pásztor E, Barnucz E, Mirk É, Van der Vusse GJ, Ligeti L, Ivanics T. (2010) Hearts of surviving MLP-KO mice show transient changes of intracellular calcium handling. *Molecular and Cellular Biochemistry*, 342:251-260. (IF: 2.168)

Miklós Zs, **Kemecsei P**, Bíró T, Marincsák R, Tóth BI, Op den Buijs J, Benis É, Drozgyik A, Ivanics T. (2012) Early cardiac dysfunction is rescued by upregulation of SERCA2a pump activity in a rat model of metabolic syndrome. *Acta Physiol (Oxf)*. 205(3):381-93 (IF: 3.09)

Other own publications

Miklós Zs, Ivanics T, Roemen THM, Van der Vusse GJ, Dézsi L, Szekeres M, **Kemecsei P**, Tóth A, Ligeti L. (2003) Time related changes in calcium handling in the isolated ischemic and reperfused rat heart. *Molecular and Cellular Biochemistry*, 250(1):115-124 (IF: 1.763)

Szenczi O, **Kemecsei P**, Miklós Zs, Ligeti L, Snoeckx LHEH, van Riel NAW, op den Buijs J, Van der Vusse GJ, Ivanics T. (2005) In vivo heat shock preconditioning mitigates calcium overload during ischaemia/reperfusion in the isolated, perfused rat heart. *Pflügers Archiv European Journal of Physiology*, 449:518-525. (IF: 3.564)

Szenczi O, **Kemecsei P**, Holthuijsen MFJ, van Riel NAW, van der Vusse GJ, Pacher P, Szabó Cs, Kollai M, Ligeti L, Ivanics T. (2005) Poly(ADP-ribose) polymerase regulates myocardial calcium handling in doxorubicin-induced heart failure. *Biochemical Pharmacology*, 69:725-732 (IF: 3.617)